Photoemission electron microscopy for connectomics

Wildenberg, G.; Boergens K.M.; Lambert, L.; Li, R.; Craig, A.; Man, M.K.L.; ... ; Kasthuri, N.

PNAS BRIEF REPORT | NEUROSCIENCE OPEN ACCESS

Photoemission electron microscopy for connectomics

Gregg Wildenberg[a,b,1], Kevin M. Boergens[c,1], Lola Lambert[a,1], Ruiyu Li[d,e], Allison Craig[e,f], Michael K. L. Man[g], Amin Moradi[h], Janek Rieger[d,e], Hengli Duan[i], Sarnjeet S. Dhesi[i], Gabriel Karras[i], Francesco Maccherozzi[i], Keshav Dani[g], Rudolf Tromp[h], Sense Jan van der Molen[h], Sarah B. King[d,e,2], and Narayanan Kasthuri[a,b,2]

Edited by Edward Callaway, University of California San Diego, La Jolla, CA; received August 8, 2025; accepted October 8, 2025

Photoemission electron microscopy (PEEM) offers a potential third modality for large-volume connectomics alongside transmission electron microscopy (TEM) and scanning electron microscopy (SEM). We image osmium stained, ultrathin brain sections on gold coated silicon at synaptic resolution using commercial PEEMs. At coarser resolution, we demonstrate that ultraviolet laser illumination enables gigavoxel-per-second acquisition rates without thermal damage. PEEM combines TEM-like parallel detection with SEM-compatible solid supports into a potentially scalable and cost-effective approach for large-volume connectomes.

Photoemission Electron Microscopy (PEEM) | connectomics | brain mapping

A confluence of advances in 3D electron microscopy (EM) imaging, sample preparation, and algorithms has enabled the mapping of how neurons connect in large volumes of brain—connectomics. Connectomics has emerged as an invaluable tool in the neuroscience armamentarium, and the analysis of wiring patterns in the cortex, hippocampus, retina, songbird sensory motor cortex, zebrafish larvae, and entire fly brains has helped discover principles of brain functions that could not have been revealed in any other way (1). These datasets are also inherently valuable as public repositories for future investigations by the broader neuroscience community. Thus, large 3D datasets at synaptic resolution will be vital to future neuroscience research, with the next leap in connectomics being the reconstruction of full neural circuits in mammalian brains. However, all EM connectomic reconstructions use either transmission electron microscopy (TEM) or scanning electron microscopy (SEM), which have limitations in the reliable automated serial pickup of ultrathin brain slices (UTBS) or in acquisition costs, respectively. To make that leap to mammalian connectomes, large-volume connectomes need to be cheaper and faster.

In this study, we investigated whether a third type of electron microscopy, photoemission electron microscopy (PEEM), could be used for high-throughput imaging of UTBS for connectomics. Photoemission electron microscopes are commercially available, are routinely used in chemistry and surface physics, and have been sporadically used since the 1970s for biological imaging (2–4) and even to image neurons in culture (5). PEEM uses wide-field illumination (such as UV light) to emit photoelectrons from materials (6). Variations in the resulting photoemission pattern are captured with standard electron optics (Fig. 1*A*). Photoemitted electrons are accelerated (usually to 10 keV to 20 keV) and projected with electrostatic and electromagnetic lenses onto an electron detector. Commercial PEEMs can have resolution capabilities as low as 5 nm (7). There are also cameras available that capture PEEM data at 10 GHz pixel rates, making a fast PEEM for connectomics plausible. Laser illumination can be used in PEEM to increase throughput compared to incoherent light sources, offering a promising approach for significantly accelerated neural circuit mapping that combines the most attractive aspects of scanning and transmission EM (Fig. 1*A*).

Results

As PEEM is usually done on flat conductive substrates, we manually picked up 60-nm-thick brain sections that had been prepared for EM-based connectomics (8) on a square-centimeter-sized piece of silicon, coated with gold, and glow-discharged to increase hydrophilicity and adhesiveness of the brain sections to the substrate. Here, we captured synaptic resolution images with a mercury arc lamp (Fig. 1*B*). We measured the resolution (*Methods*) as 20 nm, meaning PEEMs can deliver sufficient resolution for full connectomic circuit reconstruction.

Author affiliations: [a]Department of Neurobiology, University of Chicago, Chicago, IL 60637; [b]Biosciences Division, Argonne National Laboratory, Lemont, IL 60439; [c]Department of Physics, University of Illinois Chicago, Chicago, IL 60607; [d]Department of Chemistry, University of Chicago, Chicago, IL 60637; [e]James Franck Institute, University of Chicago, Chicago, IL 60637; [f]Graduate Program in Biophysical Sciences, University of Chicago, Chicago, IL 60637; [g]Okinawa Institute of Science and Technology, Femtosecond Spectroscopy Unit, Onnason, Kunigami-gun Okinawa 904-0495, Japan; [h]Leiden Institute of Physics, Leiden University, Leiden 2333 CA, The Netherlands; and [i]Diamond Light Source, Magnetic Materials Group, Didcot OX110DE, United Kingdom

Author contributions: G.W., L.L., R.L., M.K.L.M., A.M., J.R., H.D., S.D., G.K., F.M., K.D., R.T., S.J.v.d.M., S.B.K., and N.K. designed research; G.W., K.M.B., L.L., R.L., M.K.L.M., A.M., J.R., and H.D. performed research; G.W., K.M.B., L.L., A.C., and M.K.L.M. analyzed data; and G.W., K.M.B., L.L., S.B.K., and N.K. wrote the paper.

Competing interest statement: Patent #WO2024249548A2.

[1]G.W., K.M.B., and L.L. contributed equally to this work.

[2]To whom correspondence may be addressed. Email: sbking@uchicago.edu or bobbykasthuri@uchicago.edu.

Published November 24, 2025.

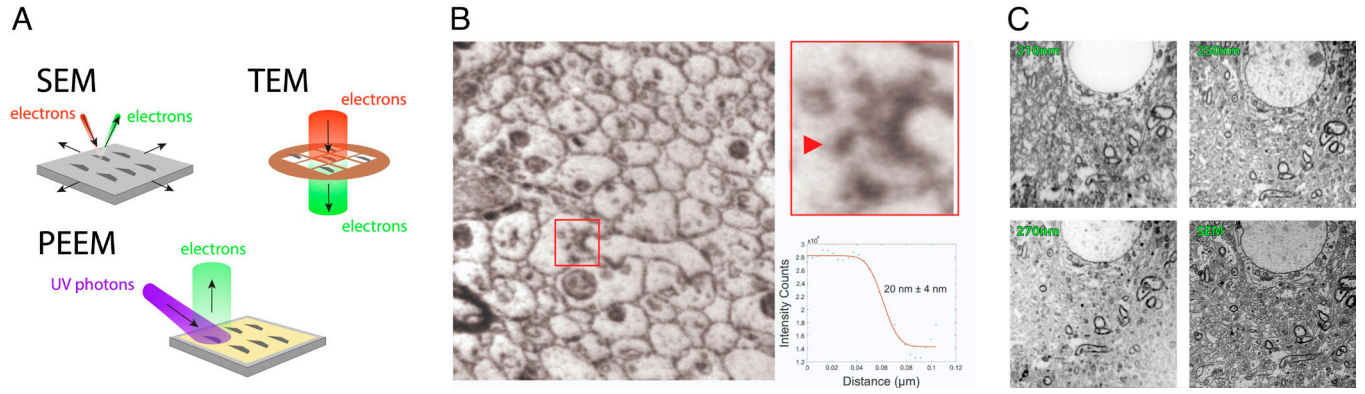

Fig. 1. (*A*) PEEM combines the advantages of SEM and TEM for high-throughput volume electron microscopy (vEM). (*B*) High-resolution PEEM image of a UTBS. (*Top Right*) We can visualize multiple synapses (red square) as evidenced by the presence of postsynaptic densities (PSD) and presynaptic vesicle clouds. (*Bottom Right*) Line cut resolution measurement. Field of view: 4.27 μm. (*C*) Dependence of PEEM images on illumination wavelength. Field of view: 20 μm.

But importantly with PEEM, throughput can be sped up considerably by increasing photon flux, via a laser. Therefore, we next investigated laser illumination of the UTBS in a PEEM. Because arc lamp light is polychromatic, we first investigated the wavelength dependence of contrast and found that with a pulsed laser, image acquisition was possible at all three wavelengths assessed (210 nm, 250 nm, 270 nm) (Fig. 1*C*). The range of possible wavelengths highlights the flexibility of using PEEM, allowing optimization in the space of electron yield and availability of lasers. For example, the ratio of incoming photons to outgoing electrons (quantum yield) was 19 times more favorable at 210 nm. However, there are more affordable, commercially available lasers at 266 nm (i.e., lower cost per electron generated), so we concentrated on the latter for further investigation.

With a 266 nm continuous-wave laser, we imaged sections at 100 ms, 10 ms, and 1 ms exposure time on a 6 μm field of view (Fig. 2). In all three cases, we could clearly see individual plasma membranes of individual neurons in neuropil, even at the relatively low laser powers used here, 28.37 mW. Additionally, we imaged small stacks with both arc lamp and 266 nm laser (9, 10) and found the reconstructability promising.

Discussion

In summary, we describe the first successful imaging of UTBS using PEEM at synaptic resolution. Furthermore, we demonstrate that UV laser illumination of UTBS significantly increases PEEM imaging rates, exceeding state-of-the-art SEM and TEM techniques used for connectomic imaging of brains. Finite element analysis shows that laser powers more than 100 times what we demonstrate in our experiments are safe without thermal damage of the sample, suggesting 1 ms images with signal to noise comparable to that of the 100 ms image are possible. Finally, initial experiments suggest that PEEM is compatible with ion milling (Fig. 2). Serial ion milling of UTBS could reveal potential limitations in the effective imaging depth of PEEM within an UTBS and the long-term stability of UTBS in PEEM imaging when combined with serial milling.

Since PEEM has similar requirements as SEM imaging (i.e., section flatness, conductive substrates, and maximizing UTBS density), we argue that existing state-of-the-art approaches for automated collection of serial UTBS on conductive substrates, such as automated collection on tape (ATUM) (11–13), and collection on silicon (MagC) (14, 15), could be used to scale the number of UTBS for PEEM.

Illuminating UTBS with photons instead of electrons opens up the space of sample preparation for PEEM imaging. With this contrast mechanism, it is plausible that different sample preparations may be even more suitable for PEEM and that combinations of existing EM stains or entirely new stains could increase contrast. Also, for each contrast agent candidate, higher throughput could be achieved by identifying the optimal excitation wavelength. Stain, laser wavelength, and milling thickness (14, 16) could be matched to extract the maximum amount of information from the sample in minimum time.

An adult mouse brain conservatively estimated to be 1 cm^3, sliced to 30 nm, imaged at 8 nm pixel size, would result in a dataset of 5.2×10^{17} voxels. A single PEEM with a UV laser, imaging nonstop at a net 2 GHz pixel rate (Fig. 2), would take approximately 8.2 y. Commercially available PEEM instruments could be used to do high-throughput connectomics imaging, needing only software modifications and a stage that can hold and address a large wafer. Additionally, UTBS can be easily distributed across multiple PEEMs, decreasing the time to map a mouse brain proportionately to the number of PEEMs used. Looking forward, a 10 GHz PEEM is plausible given the analyses above and would pave the way for even larger mammalian brains.

Methods

Sample Preparation. Mouse brain sections were prepared for PEEM imaging following the same protocol used for standard SEM preparation using multiple rounds of osmium tetroxide staining (8). In brief, the mouse was perfused transcardially to preserve the ultrastructure. The mouse brain was surgically removed, postfixed, and a vibratome-sectioned brain slice (200 to 300 μm) was stained with successive rounds of osmium tetroxide, potassium ferrocyanide, uranyl acetate, and lead nitrate, before ethanol dehydration and embedding with EPON resin. Resin-encapsulated brain was then sliced using an ultramicrotome to 40 to 60-nm-thick UTBS, which were picked up on a Si substrate (coated with gold and glow-discharged). Samples for Fig. 2 received an ion beam treatment, for details, see below.

For Fig. 1*B*, the UTBS on the substrate was illuminated using a broadband mercury arc lamp with a short pass filter allowing photons with energies greater than 4.43 eV (280 nm) to arrive on the sample. The resulting photoelectrons were imaged with a photoemission electron microscope manufactured by SPECS GmbH [aberration-corrected microscope (7)]. The typical exposure time for one image was hundreds of seconds. High-resolution images are obtained by integrating the same region of interest to improve signal-to-noise.

The PEEM image in Fig. 1*C* was acquired using an aberration-corrected spectroscopic photoemission and low-energy electron microscopy system (AC-SPELEEM Elmitec GmbH). Energy-resolved PEEM measurements were performed by coupling the PEEM with a Yb-doped fiber amplifier laser system, which delivered 230 fs, 1,030 nm pulses at a 4 MHz repetition rate. The tunable laser generated photons with wavelengths of 210 nm, 250 nm, and 270 nm using a noncollinear optical

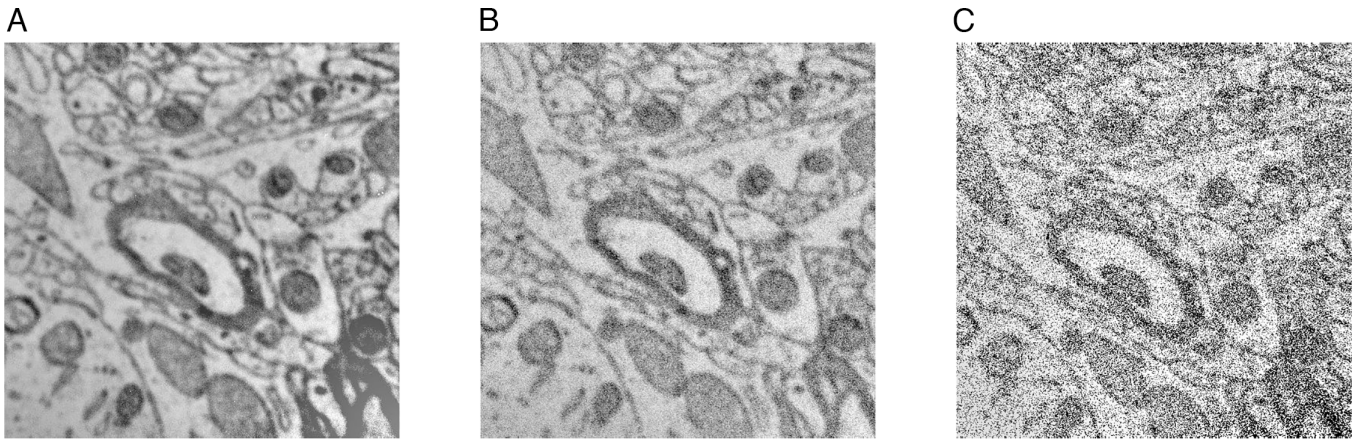

Fig. 2. Micrographs of UTBS taken with decreasing exposure time, illuminated with a 266 nm continuous-wave laser at constant power, with a fluence of 0.04 milliwatts/μm^2. For a 10 Megapixel camera, this corresponds to a raw throughput of 0.1 (*A*), 1 (*B*), 10 (*C*) Gigavoxel per second, respectively. Field of view: 6 μm.

parametric amplifier. An energy slit was applied in the energy analyzer, providing energy-resolved images with an approximate energy resolution of 250 meV.

To ensure operation below the vacuum space charge limit–where image blurring and energy spectrum broadening are avoided–we used an energy density of 230 nJ/cm^2. The laser spot size on the sample was larger than 100 μm. PEEM images were acquired with an exposure time of 16 s per frame and averaged over sixty frames after applying flat-field, dark-field, and drift corrections.

The sections were stained and sliced as above, then picked up on 10 mm by 10 mm silicon chips coated in 100 nm of gold (MSE Supplies, AZ, US). The sections were then polished on a Scia 150 with the following parameters before imaging: source start of 270 W, beam voltage of 400 V, accelerator voltage of 700 V, and neutralizer current of 200 mA. The sample temperature was set to 15 °C, and 7 standard cubic centimeters per minute (sccm) of helium was ran through the sample holder to cool the samples. Argon 1 was set at 7 sccm, and Argon 2 was set at 12 sccm. The sample angle was set at 10°, and the sample was rotated at 5 RPM.

The sections were illuminated using a 266 nm continuous wave laser and imaged with an PEEM (Elmitec GmbH). The laser spot size was approximately 30 μm in diameter. The laser power was measured using a laser power meter placed in front of the beam. The PEEM image detector used was a CheeTah quad detector with Medipix3 (Amsterdam Scientific Instruments, NL).

Finite Element Analysis of Heating. Finite element analysis was performed using COMSOL Multiphysics 5.2.0 to model the thermal response of the diamond substrate under laser illumination. The substrate was modeled as diamond with a thermal conductivity of 1,500 W/m/K, consistent with commercially available polycrystalline CVD diamond wafers. Laser heating was simulated assuming uniform illumination over a circular area of 40 μm diameter with 100% optical absorption. Thermal boundary conditions included a fixed temperature heat sink at the bottom surface of the diamond wafer, representing the primary thermal conduction pathway, while all other surfaces were treated as thermally insulated. Steady-state conditions were assumed for all calculations, allowing the system to reach thermal equilibrium under continuous laser excitation.

Resolution. We took a linecut over a small region of the image and fit the photoemission intensity. Spatial resolution is calculated as the distance between 16% and 84% of the error function, corresponding to the SD of a Gaussian instrumental response convoluted with a Heaviside step function.

Data, Materials, and Software Availability. 3D image stacks data have been deposited in Webknossos [https://webknossos.org/links/iyQBZLZFmxtDAe8e (9) and https://webknossos.org/links/gMXAns5EtQo89QVU (10)].

1. J. Kornfeld, W. Denk, Progress and remaining challenges in high-throughput volume electron microscopy. *Curr. Opin. Neurobiol.* **50**, 261–267 (2018).
2. E. Bauer, A brief history of PEEM. *J. Electron Spectrosc. Relat. Phenom.* **185**, 314–322 (2012).
3. R. Könenkamp *et al.*, 5.4nm spatial resolution in biological photoemission electron microscopy. *Ultramicroscopy* **110**, 899–902 (2010).
4. A. Skallberg, K. Bunnfors, C. Brommesson, K. Uvdal, New tools for imaging neutrophils: Work function mapping and element-specific, label-free imaging of cellular structures. *Nano Lett.* **21**, 222–229 (2021).
5. G. de Stasio *et al.*, High-resolution photoelectron microimaging of neuron networks. *Europhys. Lett.* **16**, 411 (1991).
6. R. Li *et al.*, OsO2 as the contrast-generating chemical species of osmium-stained biological tissues in electron microscopy. *Chembiochem* **25**, e202400311 (2024).
7. R. M. Tromp *et al.*, A new aberration-corrected, energy-filtered LEEM/PEEM instrument. I. Principles and design. *Ultramicroscopy* **110**, 852–861 (2010).
8. Y. Hua, P. Laserstein, M. Helmstaedter, Large-volume en-bloc staining for electron microscopy-based connectomics. *Nat. Commun.* **6**, 7923 (2015).
9. K. M. Boergens, webknossos Hg Arc lamp PEEM image stack. WebKnossos. https://webknossos.org/links/iyQBZLZFmxtDAe8e. Deposited 7 August 2025.
10. K. M. Boergens, webknossos Laser PEEM *image* stack. WebKnossos https://webknossos.org/links/gMXAns5EtQo89QVU. Deposited 7 August 2025.
11. N. Kasthuri *et al.*, Saturated reconstruction of a volume of neocortex. *Cell* **162**, 648–661 (2015).
12. Y. Kubota *et al.*, A carbon nanotube tape for serial-section electron microscopy of brain ultrastructure. *Nat. Commun.* **9**, 437 (2018).
13. V. Baena, R. L. Schalek, J. W. Lichtman, M. Terasaki, Serial-section electron microscopy using automated tape-collecting ultramicrotome (ATUM). *Methods Cell Biol.* **152**, 41–67 (2019).
14. T. Templier, MagC, magnetic collection of ultrathin sections for volumetric correlative light and electron microscopy. *Elife* **8**, e45696 (2019).
15. K. A. Fulton, P. V. Watkins, K. L. Briggman, GAUSS-EM: Guided accumulation of ultrathin serial sections with a static magnetic field for volume electron microscopy. *Cell Rep. Methods* 4, 100720 (2024).
16. H. Ma *et al.*, PIBE: Parallel ion beam etching of sections collected on wafer for ultra large-scale connectomics. BioRxiv [Preprint] (2025). https://www.biorxiv.org/content/10.1101/2025.04.25.650569v2 (Accessed 9 September 2025).